NIKE - PULSELINE AND DIODE DESIGN FOR THE 60 cm AMPLIFIER

P. A. Corcoran, I. D. Smith, R. G. Altes, M. J. Christensen, B. D. Chugg
Pulse Sciences, Inc., 600 McCormick St., San Leandro, CA 94577

M. W. McGeoch
ARL (Textron Defense Systems), 2385 Revere Beach Parkway, Everett, MA 02149

J. D. Sethian, S. P. Obenschain
Naval Research Laboratory, Plasma Physics Div., Washington, D.C. 20375

R. L. Morse
Commonwealth Technology, Inc., 5875 Barclay Drive, Alexandria, VA 22310

ABSTRACT

An identical pair of pulsed power systems has been designed to drive the 60 cm aperture amplifier as part of the Naval Research Laboratory's NIKE KrF laser system. The KrF gas volume is pumped from two opposite sides by 60 cm x 200 cm electron beams which are produced by two totally independent systems. Each pulse power system includes a ~ 240 kJ Marx, four (parallel) 5 ohm water filled coaxial pulseforming lines (PFLs), four laser triggered output switches and a monolithic, magnetic field immersed diode. Prominent design features include the large area of the water lines, 90° bends in the PFLs, radial-plastic output switch diaphragms (as in SUPER-SPRITE at RAL), and inside/out vacuum bushings (as in AURORA at LANL). Triggered diverters and various passive eleents were designed to reduce damage in the event of a fault. A 4 ohm peaking section directly precedes the output switches to increase the flat top duration and an anode field shaper has been designed to reduce e-beam halo in the diode. Detailed circuit simulations show each system will produce a 700 keV, 100 kJ, 250 ns electron beam when driving a matched 1.25 ohm diode. Electrical stress and breakdown fractions were calculated throughout. The diode was modelled analytically and with an electron transport code. In the circuit code, the diode was represented by a Child-Langmuir model whose gap closes at 2.5 cm/μs. The transient response of the 90° bends in the PFLs was determined by a fully 3-D transmission line simulation as well as by a scaled analog model. Hardware fabrication is scheduled to begin in August 1991 with the goal of having one pulse power system (one-half the amplifier) operational by April 1992. The full 60 cm amplifier system is scheduled to be on-line by April 1993.

INTRODUCTION AND OVERVIEW

The Naval Research Laboratory's (NRL's) NIKE KrF laser system[1] is designed to address physics and technical issues for direct-drive laser fusion. NIKE is expected to deliver greater than 3 kJ on target with a 1% uniformity in the focal profile using Eschelon-free ISI beam smoothing technology[2]. A shot rate of greater than 1000/year is desired.

The double-pass 60 cm aperture amplifier is the final e-beam pumped amplifier in a system which includes a 20 cm amplifier[3] (just prior), several preamps and an oscillator. Its 60x56x200 cm^3 gas volume is pumped from two opposite sides in order to achieve a more uniform energy deposition.

A plan view of the 60 cm amplifier is shown in Figure 1. It shows the amplifier's KrF gas volume flanked on each side by a diode, four coaxial pulseforming lines, and a Marx generator. The systems on each side are identical mirror-images except for a handful of minor mechanical details. Each pulseforming line was bent 90° in order to fit within a predefined building. The oil filled coaxial feed lines which connect the Marx to each PFL are staggered in length since each water filled PFL has the same length. The coplanar coaxial lines are supported by carts at a common centerline height of 66 inches above the floor. The Marx tanks and pulselines are on roller-bearings and tracks to allow the entire system on each side of the amplifier to be rolled away to expose the diode and output switches for easy assembly and maintenance. System 1 in Figure 1 is shown in its rolled away maintenance position while System 2 is fully assembled.

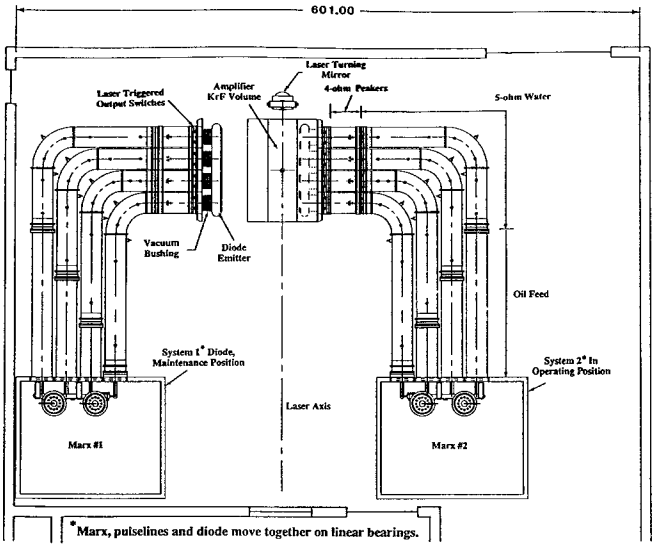

Figure 1. Plan view of 60 cm amplifier.

The specified operating modes for each side of the 60 cm amplifier are shown in Figure 2. Combined, the two sides will deliver between 170 kJ and 200 kJ depending on the option. The pulseline design was done for the highest stress "high power" option shown.

This work was supported by the U.S. Department of Energy.

Report Documentation Page

Form Approved
OMB No. 0704-0188

1. REPORT DATE	2. REPORT TYPE	3. DATES COVERED
JUN 1991	**N/A**	**-**

4. TITLE AND SUBTITLE	5a. CONTRACT NUMBER
Nike- Pulseune And Diode Design For The 60 Em Amplifier	5b. GRANT NUMBER
	5c. PROGRAM ELEMENT NUMBER
6. AUTHOR(S)	5d. PROJECT NUMBER
	5e. TASK NUMBER
	5f. WORK UNIT NUMBER
7. PERFORMING ORGANIZATION NAME(S) AND ADDRESS(ES) **Pulse Sciences, Inc., 600 McCormick St., San Leandro, CA 94577**	8. PERFORMING ORGANIZATION REPORT NUMBER
9. SPONSORING/MONITORING AGENCY NAME(S) AND ADDRESS(ES)	10. SPONSOR/MONITOR'S ACRONYM(S)
	11. SPONSOR/MONITOR'S REPORT NUMBER(S)

12. DISTRIBUTION/AVAILABILITY STATEMENT
Approved for public release, distribution unlimited

13. SUPPLEMENTARY NOTES
See also ADM002371. 2013 IEEE Pulsed Power Conference, Digest of Technical Papers 1976-2013, and Abstracts of the 2013 IEEE International Conference on Plasma Science. Held in San Francisco, CA on 16-21 June 2013. U.S. Government or Federal Purpose Rights License

14. ABSTRACT
An identical pair of pulsed power systems has been designed to drive the 60 em aperture amplifier as part of the Naval Research Laboratory's NIKE KrF laser system. The KrF gas volume is pumped from two opposite sides by 60 em x 200 em electron beams which are produced by two totally independent systems. Each pulse power system includes a - 240 kJ Marx, four (parallel) 5 ohm water filled coaxial pulseforming lines (PFLs), four laser triggered output switches and a monolithic, magnetic field immersed diode. Prominent design features include the large area of the water lines, 90Â° bends in the PFLs, radial-plastic output switch diaphragms (as in SUPER-SPRITE at RAL), and inside/out vacuum bushings (as in AURORA at LANL). Triggered diverters and various passive eleents were designed to reduce damage in the event of a fault.

15. SUBJECT TERMS

16. SECURITY CLASSIFICATION OF:			17. LIMITATION OF ABSTRACT	18. NUMBER OF PAGES	19a. NAME OF RESPONSIBLE PERSON
a. REPORT	b. ABSTRACT	c. THIS PAGE			
unclassified	**unclassified**	**unclassified**	**SAR**	**6**	

Option*	Beam Parameters	Diode (V)	Diode (I)	PFL Charge (V)
Baseline	333 GW @ 1.25 Ω	645 kV	516 kA	1290 kV
High Power	392 GW @ 1.25 Ω	700 kV	560 kA	1400 kV
High Impedance	326 GW @ 1.50 Ω	700 kV	466 kA	1283 kV
Low Impedance	386 GW @ 1.00 Ω	622 kV	622 kA	1399 kV

*All options assume a 250 ns pulse length measured at 90% peak power and a 1.25 ohm driver formed by four pulselines at 5 ohms each.

Figure 2. NIKE operating options.

CIRCUIT

The complete circuit for one side of the amplifier is shown in Figure 3. The Marx charge voltage and diode impedances are set for the high power option. The Marx has not been designed but is assumed to be 12 stages each with four series-parallel 2.8 μF, 60 kV capacitors, which are available at NRL. The Marx capacitance is initially charged to 1320 kV which corresponds to a comfortable 55 kV charge on the capacitors (92% of their rated voltage). The Marx clamp is normally open in this circuit unless the prefire fault is being studied. The PFLs are 165 ns long with a nominal impedance of 1.25 ohms (=5 Ω/4), the impedance of the last 20 ns is 1 ohm (=4 Ω/4) to hasten the output risetime. The PFLs are charged through a busbar, 2 ohm isolation/damping resistors, and 1.2 μH isolation inductors. The isolation inductors are formed by the elements shown in the oil coaxes except for the shortest one which has an inductive element added to its end of the busbar. The SF_6 output switches close at 1.7 μs and the two divertor switches (attached to the busbar) normally close 165 ns later, a PFL transit time. The diverter switches each have a closed resistance of 3 ohms. The diode resistance is calculated using the nonrelativistic Child-Langmuir model. The initial diode gap is 5.0 cm and closes with a velocity 2.5 cm/μs. The diode has a 1.25 ohm matched impedance at the middle of the useful power pulse.

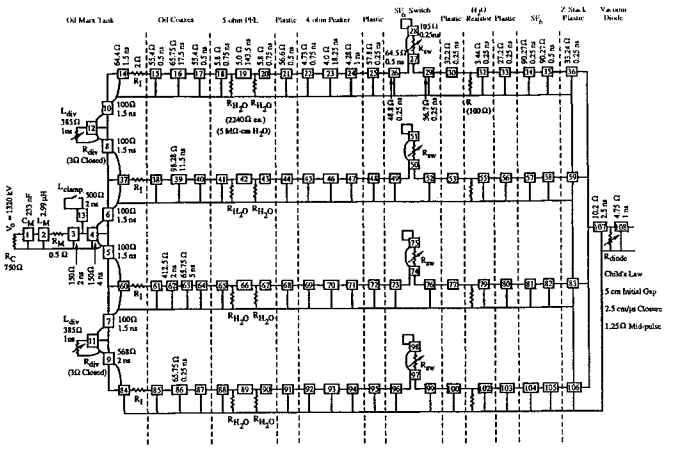

Figure 3. NIKE circuit diagram for one side of amplifier.

The diode power predicted by this model, Figure 4, has an amplitude of 387 GW ± 5% and is 253 ns at 90% of its peak. The diode voltage, also shown, has an amplitude of 671 kV ± 5% during the same 253 ns. The circuit performance was simulated using PSI's transmission line code TLCODE[4]. The fundamental time step was 0.25 ns.

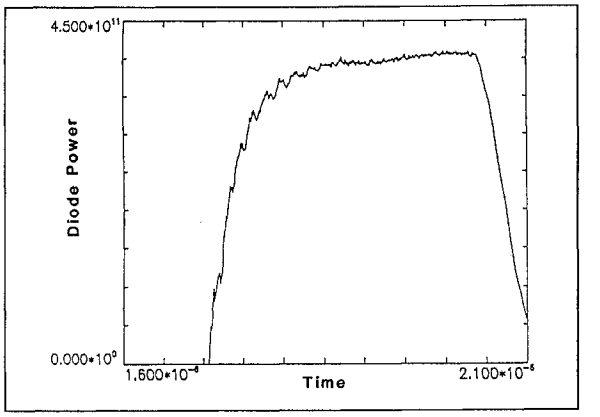

Amplitude = 387 GW ± 5%
Pulsewidth = 253 ns at 90% peak power

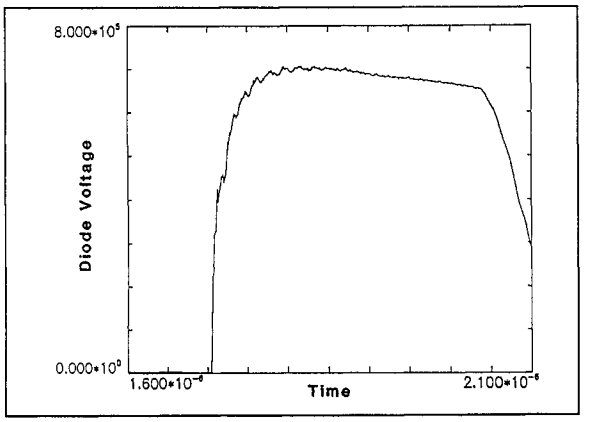

Amplitude = 671 kV ± 5% during same 253 ns

Figure 4. Diode power and voltage for high power option.

KEY COMPONENTS

Marxes. Each Marx is an oil-insulated twelve-stage unit with a maximum erected (open circuit) voltage of 1440 kV and stored energy of 240 kJ at full charge. As the Marx design has not yet been finalized, there is some uncertainty in the Marx configuration and consequently the Marx inductance. However, the water line stress limits the Marx inductance to less than 4.8 μH, and concessions to reality prescribe the inductance to be greater than 2.7 μH. This full range of inductance was modelled to determine the effect on the PFL charging time.

Oil Lines. The high voltage terminal of each Marx is attached to the midpoint of a busbar which in turn charges each PFL through an isolation inductor and resistor (1.2 μH and 2 ohms). The isolation elements were designed to both maintain the voltage on other PFLs and damp inter-PFL currents if one PFL were to break down. The isolation inductor feeding each line was formed differently in order to accommodate the different lengths of oil filled coax. By picking the proper impedance, the isolation inductance was completely formed by the oil coaxes on the two longest lines, while additional discrete inductors were needed for the two shorter ones (Figure 3). The isolation resistors are shown as salt-water filled plastic tubes which span the gap from the busbar to the oil coaxes. Balanced inductance and resistance in these feeds assure that each water line charges equally.

Two triggered diverter switches are located in each Marx tank to prevent the water line stress from approaching breakdown levels in

the event that a Marx prefires after the dc clamp is removed or that a normal triggered firing of the Marx is followed by the failure of the output switches to close. Also, in a completely normal firing, the diverters will reduce the post-pulse voltage and current to prevent damage to the anode foil or wires in the diode. The 1.4 MV switches will be patterned after the Saturn (SNLA) rim fire switches (2.5 to 3 MV, 500 kA, 25 kJ/ohm)[5] and will consist of a 1 MV trigatron and only five stages. The 36 switches in Saturn have demonstrated a reliably low jitter of about 10 ns first to last. For access and ease of removal, the switches are placed above the busbar and attached to the Marx support structure at the top of the tank. The vertical switch axes keep debris off the envelopes and make access easy for the trigger cables. Each switch is in series with an array of salt-water filled tubes whose total resistance is nominally 3 ohms.

Water Lines. Each water filled PFL has a single transit time of 165 ns (553 cm) and has a 5 ohm impedance for all but the last 20 ns, which is a risetime peaker, and has a impedance of 4 ohms. The outer conductor of the PFL is to be made of standard 20 inch diameter, thin walled stainless steel pipe; the inner (electrical) surface of this pipe has a 19.56 inch diameter. The PFL has an open circuit time to peak of 1.9 μs but was switched in the circuit simulations at 1.7 μs to offset the voltage droop caused by the assumed 2.5 cm/μs diode gap closure. Figure 5 shows typical charging waveforms at the high power operating level for a normal shot and one in which the output switches fail to fire and the lines are relieved by the diverter switches. The two waveforms are measured at opposite ends of the PFL to show the maximum stress in each case. Ian Smith's water breakdown formulas as modified by NRL[6], were used to calculate the electrical stress in the PFLs since the combined surface area of all eight PFLs was 691 k cm^2 for the outers and 334 k cm^2 for the inners. For the normal high power shot (Figure 5(a)), these calculations predict a 62% breakdown fraction on the electrically weaker positive outer conductors in the 5 ohm sections of the PFL and 65% on the 4 ohm peaker section. The breakdown fractions for the no-output switch diverter only fault mode are 71% and 89% respectively. Though acceptable as they are, it is comforting that there is an extra margin of safety for the fault mode fractions since the effective time is ~1.2 μs while the formulas were derived for times ≤ 1 μs and the time dependance is known to gradually decrease as the applied voltage duration increases.

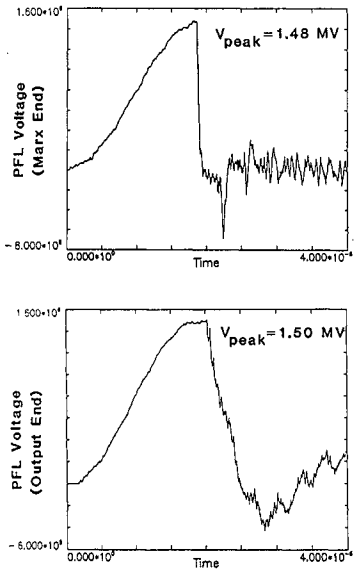

Normal Shot

τ_{os} = 1.7 μs

$\tau_{div} = \tau_{os}$ + 165 ns

Faulted Shot

- No output switch fire
- Diverters only

τ_{div} = 1.7 μs + 165 ns

Figure 5. PFL charging waveforms for high power operating level.

Bends. The main design issue for the bends was their effect on the output pulse shape since the diode power was required to be flat to within ± 5%. The outer conductors of the 90° bends in the PFLs are 20 inch diameter to match the rest of the PFL and are specified as standard elbows with a centerline bend radius of 30 inches. It was relatively easy to determine that the field enhancements in the bend had a negligible effect on the PFL's overall breakdown fraction, especially since the affected surface areas were small. The concern was that the bends would reflect a significant part of the discharge transient. Although the effect of a single bend will be roughly quartered by the staggered distances of the bends from the diode in order to determine the size of the reflections, both computer and analog work was performed.

The computer based measurements were made using TL3D; a fully 3-D simulator based on the transmission line (circuit) code TLCODE. The computational mesh was cubic, and had a 77 ps transit time between nodes, and was generated directly from physical dimensions. The analog model was constructed from standard 3 inch diameter copper pipe for the outer and 1.5 inch diameter for the inner. The pulses were generated and measured by a Tektronix 7512 unit with an S-6 sampling head and an S-52 pulse generator.

The computer and analog measurements agreed and lead to the conclusion that, with a 50 ns risetime and the staggering, the predicted perturbations due to the bends will be negligible in the full system. A much faster risetime would be needed in order to see significant perturbations, for example a 7.1 ns 10-90% risetime injected into the computer model produced ± 2.3% reflections from the bend itself and a 12% over-shoot on the pulse reflected from the model's open circuit end.

Output Switches. Each output switch, as shown in Figure 6, consists of a single SF_6 gas insulated, laser triggered spark gap. The SF_6 volume is contained by radial plastic diaphragms and by a coaxial metal cylinder. This unusual switch geometry was patterned after the switches used in RLA's Super Sprite[7] and NRL's Poseidon[8]. The switch has a 4 cm gap which is adjustable ± 1/2 cm by shimming the downstream electrode. The total inductance for a single switch is 102 nH including the two adjacent diaphragms.

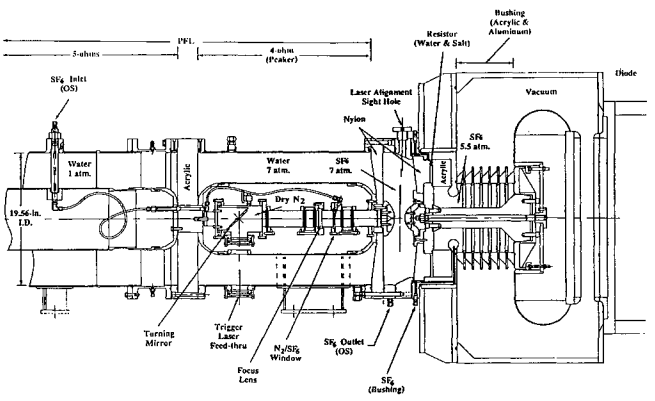

Figure 6. Output end of PFL and diode.

The switches are expected to be triggered at 65% of self- break with a pressure of 100 psi for the high power option (1.4 MV PFL charge). Each switch will be triggered by a 11.3 mJ, 266 nm (frequency quadrupled Nd:YAG) laser pulse whose focussed power density will be roughly 5 GW/cm^2. The switch is expected to have a jitter in the range of 0.8 to 1.7 ns (1σ). The self-break expectations were extrapolated from tests performed on the SLIA Injector

switches[9], and the jitter from the accumulated measurements made by PSI, SNLA, LANL and NRL[3, 8, 9, 10].

The trigger laser enters the side of the peaker section through a saphire window, and crosses the water to a light tube located inside the peaker's inner conductor. The first part of the light tube is filled with a captive volume of dry nitrogen and contains a turning mirror and a focusing lens. The nitrogen to SF_6 boundary is a saphire window which will be located at a distance of 25 cm from the spark gap. This window can be spoiled by switchout by-products so it is flushed by the SF_6 injected through a hollow plastic tie rod located back in the 5 ohm part of the PFL. Flanges on the light tube will allow the N_2/SF_6 window to be moved to almost double its distance from the switch should it require excessive maintenance.

The radial diaphragm geometry was chosen because it offered several advantages over the more conventional axial cylinder insulator geometry. The plastic diaphragms are a relatively large distance from the arc and should be less affected by the arc's hot gas and UV. Particulate switch debris will benignly fall on the outer metal cylinder, not on an insulator although any accumulation at the triple point may be a problem. The laser alignment is easily sighted through the gas and is not obscured or blocked by the insulator. The switch electrodes are easily accessed for maintenance by unbolting the outer metal cylinders and rolling the up-stream side away with the PFLs while the downstream side stays attached to the bushing/ diode assembly. The SF_6 is vented directly to the outside. And finally, this geometry offers a relatively low inductance (short length) compared to some cylindrical insulator geometries.

The primary disadvantage to the radial diaphragm switch is that an insulation failure results in a short to ground rather than to the resistors and diode downstream. Such a failure while near peak voltage could cause damage to the hardware. Several measures have been taken to minimize the risk of such a failure and to limit the damage should one still occur. The fields along the insulator surfaces have been electrostatically graded to be roughly uniform, the metal near the triple points is rounded to prevent arc initiation, and the triple points are vented to remove trapped air. The critical stresses will occur on the upstream diaphragm before the switch closes. The peak fields at the full 1400 kV charge voltage are shown on the equipotential plot in Figure 7. The water side fields were graded by slanting the plastic surface (i.e. using the dielectric discontinuity) to overcome the 1/r coaxial grading. The SF_6 side is also well graded by its proximity to the water interface. The 85 kV/cm peak SF_6 side field is about 70% of the field of an alternative switch design that had an axial diaphragm. Both upstream and downstream switch diaphragms will be made of nylon which is much tougher (shatter proof) than acrylic to limit the damage should a flashover occur.

The assembly of the peaker and the upstream half of the switch will be done on a bench where the alignment of the laser feed can be made prior to its installation within the pulseline.

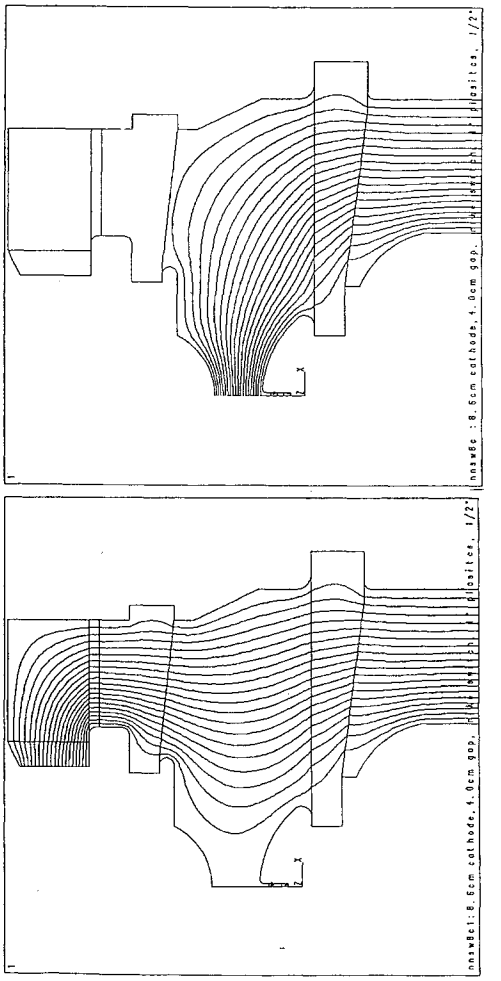

Figure 7. Equipotential plot of output switch.

Vacuum Bushing. The output switch is followed by a 100 ohm salt water filled radial resistor, an acrylic transition block, an SF_6 feedthru into the diode box and a cylindrical vacuum bushing. Each vacuum bushing is assembled from seven 1 inch thick acrylic rings with 45° vacuum angles and six 1/4 inch thick metal gradient rings. The so called "inside out" bushing design has been used in Aurora at LANL.

The peak fields (by electrostatic calculation) in the SF_6 feedthroughs are 208 kV/cm for 700 kV applied and the stack is graded within ± 13% of uniform. The voltage pulse calculated from the circuit model at the high power operating level indicates the SF_6 feedthroughs reaches 60% of self-break at a gas pressure of 75 psia and the insulator stack reaches a 53% breakdown fraction according to the standard formula $175 = Ft^{1/6} A^{1/10}$ using the combined area of the full system's eight bushings. A formula more conservative for longer pulses ($120 = Ft^{1/4} A^{1/10}$) suggests 69% of breakdown.

The inside-out bushing geometry was chosen because it is compact and it tends to put less inductance between it and the diode. It therefore has less voltage spike and ringing during the rise than more common axial and radial insulator geometries. The salt ring is used to suppress the amplitude of the prepulse and was set to minimum length (1/4 ns) in order to minimize the ringing.

A rod, which is accessed by removing the downstream switch electrode, allows a single insulator stack to be removed for servicing without having to demount the diode's cathode structure.

Diode. The diode design, illustrated in Figure 8, is given for the mid-range power of 360 GW, at 615 kV. The corresponding 585 kA curent yields 45 A/cm^2 over an area of 200 x 65 cm. A carbon felt or velvet cathode will be used. For pulse durations in the 1-5 μs range a body of data now exists for felt cathodes showing that the diode closure velocity increases as a function of the magnetic guide field[11,12], approximately as 1.6 $\sqrt{B}$ cm μs with B in kG. There is evidence however from the impedance history of the 20 cm NRL amplifier that rather lower closure velocities may apply during the first 250 ns with velvet cathodes[13]. Lower closure velocities have also been reported by Coogan, et al., in the present conference[14].

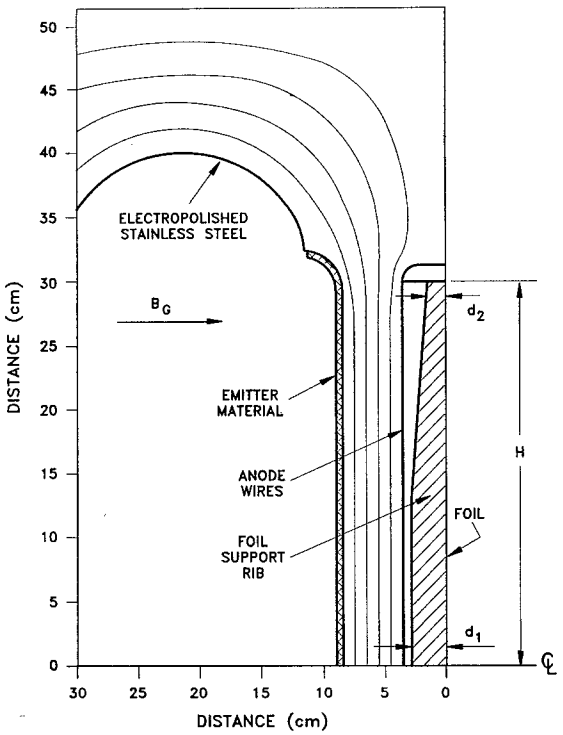

Figure 8. Cross-section of half diode.

Ideally, emission is completely confined to the emitter material and does not spread to the nearby electrode surround, or initiate at other places on the electrode. If electro-polished stainless steel is used as the electrode material, then field emission will be absent[12] at surface stresses up to 100 kV/cm and the surface gas content available to initiate discharge-type surface plasmas will be as low as can be practically achieved in a vacuum system working at 10^{-5} torr. The surface stresses are 70 kV/cm on the electrode radii along the straight sides, rising to 102 kV/cm at the four corners. The corners represent 4% of the total electrode area and have a path length to ground along the magnetic field lines of about 20 cm, so that current from the corners should be negligible. At the edge of the emitter the electrode stress is less than 50 kV/cm due to the combined effect of a rolled-back emitter and a projecting anode. The projecting anode does not degrade electron trajectories as determined using the code EGUN[15], and does not contribute additional drift length provided that its depth is much greater than the hibachi rib depth (4 cm in this design). The emitter roll-back is essential (a) to avoid an intense beam edge "halo" caused by the lack of space charge shielding beyond the edge of the beam, and (b) to form a low stress barrier region between the emitter and the rest of the electrode. The emitter is taken out to 2 cm beyond the edge of the anode aperture because electrons emitted from the roll-off region would be poorly transmitted through the hibachi due to their high angle trajectories. In this diode, with four current feeds distributed along its length, beam "rotation" is small and confined to the end regions, where it reaches a maximum vertical displacement of 1.4 cm.

The space charge limited current density, J, that can be drawn in the diode is a function of the distance, x, from the diode centerline. A guide magnetic field B_G is modified by the horizontal self-field component μo Jx to give a resultant beamlet which is angled to the cathode normal direction. Because there is an increase in electron path length the current density at height x is reduced by the factor

$$\alpha = \left[1+\left(\frac{\mu_o J x}{B_G}\right)^2\right]^{-1/2}$$

In addition, the angled rays increasingly intersect the foil support ribs, a loss which is reduced in this design by the use of tapered ribs. For ribs of depth d_1 at the centerline and d_2 at the support point, of thickness δ, separation h and half-length H, the spatially dependent part of the transmitted current density at distance x from the centerline is:

$$J(x) = \alpha J_o\left\{1-\frac{1}{h}\left(\delta + 2\,r_G + \frac{\mu_o J_o x}{B_G}\left[d_1 - \frac{(d_1-d_2)x}{H}\right]\right)\right\}$$

in which r_G is the electron gyro-radius and J_o is the cathode current density at the centerline. The gyro-radius is probably time-dependent, being related to the separation of emission sites at early times, but decreasing to near zero once a smooth plasma front has formed. For the NIKE design h = 0.076, d_1 = 0.038, d_2 = 0.020, H = 0.30, δ = 0.005, r_G = 0.002 (est.) and J_o = 45 x 10^4 (MKS). The normalized current density J/J_o is plotted in Figure 9 for a range of guide field values (anode and foil losses not included).

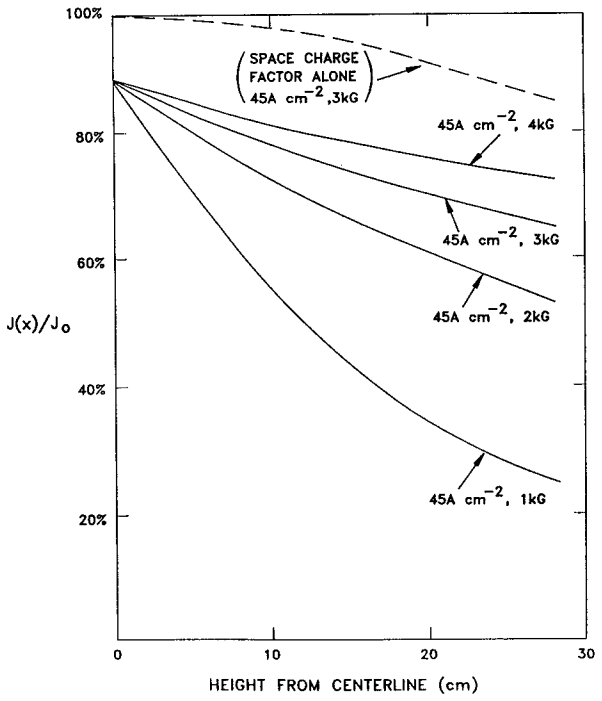

Figure 9. Spatially varying transmission factor as a function of magnetic guide field, not including edge loss, anode loss or foil loss.

The spatially independent transmission losses that are due to the overlap of the emitter with the drift aperture and the anode wire

interception, each constitute a factor of 0.92. The behavior of the beam once it enters the foil has to be calculated using a deposition code such as TIGER[16]. There is, for example, a higher fraction of reflected energy from a Krypton rich mixture than one rich in Argon.

ACKNOWLEDGEMENT

The authors wish to thank J. Shipman and C. Pawley for many useful discussions.

REFERENCES

[1] S. Bodner et al, *Proceedings of the Twelfth International Conference on Plasma Physics and Controlled Nuclear Fusion Research*, 3, (1990) 81.

[2] R.H. Lehmberg and J. Goldhar, *Fusion Tech.*, 11, 532 (1987).

[3] C.J. Pawley, et al., *Proceedings of "Lasers 90"* Conference, San Diego, CA., December 12-15, 1990 (to be published).

[4] W. N. Weseloh, *Proceedings of the Seventh IEEE Pulsed Power Conference*, edited by B. Bernstein and R. White (Institute of Electrical and Electronic Engineers, N. Y. 1989), p. 989.

[5] B.N. Turman and D.R. Humphreys, *Proceedings of the 6th IEEE Pulsed Power Conference*, Arlington, VA, June 1987, pp. 347-353.

[6] R.A. Eilbert, W.H. Lupton, NRL internal report.

[7] G.J. Hirst, R. Bailly-Salins and M.J. Shaw, *"Pulsed Power Development for the Supersprite Multikilojoule KrF Laser,"* Rutherford Appleton Lab., Chilton, Didcot, UK, Presented at the Eighth IEEE International Pulsed Power Conference, June 17-19, 1991, San Diego, CA.

[8] J.D. Sethian, unpublished data, 1986.

[9] J. Fockler, et al., Pulse Sciences, Inc., with M. Parsons, and L. Early, LANL, *"A 4 MV ±1% Flat-Top Electron Diode Driver"*, presented at the 8th IEEE International Pulsed Power Conference, June 17-19, 1991, San Diego, CA.

[10] G.J. Denison, et al., Sandia National Labs, Albuquerque, NM, *"A High-Voltage Multistage Laser-Triggered Gas Switch"*, presented at the 1987 Pulse Power Conference.

[11] *Visible (XeF) Laser Scale Up*, Final Technical Report for Contract DAAK40-79-C-0197, ARL Inc. (1982).

[12] M.W. McGeoch (unpublished).

[13] C.J. Pawley, et al., *Cleo 1991 Technology Digest Series*, 10, 276 (1991).

[14] J.J. Coogan, R.P. Shurter and E.A. Rose, Paper LA-UR 90-3985, 8th IEEE International Pulsed Power Conference, 1991

[15] W.B. Herrmannsfeldt, *"EGUN--An Electron Optics and Gun Design Program"*, Stanford Linear Accelerator Center, Stanford University, CA., prepared for DoE under Contract DE-AC03-76SF00515, Report No. 331, October 1988.

[16] J.A. Halbleib, Sr. and W.H. Vandevender, *Nucl. Sci. Eng.* 57. 94 (1975).